Glycoconjugate Journal 17, 283–299, 2000

Modeling ganglioside headgroups by conformational analysis and molecular dynamics

Paola Brocca[2], Anna Bernardi[1]*, Laura Raimondi[1]* and Sandro Sonnino[2]

[1]*Università di Milano (Italy), Dipartimento di Chimica Organica e Industriale, via Venezian 21, I-20133 Milano,*
[2]*Università di Milano (Italy), Dipartimento di Chimica e Biochimica Medica, via Fratelli Cervi 93, I-20090 Segrate (Milano)*

The conformations and dynamics of gangliosides GM1, GM2, 6′-GM2 and GM4 have been studied by computational means, and the results compared to NMR data. Unconstrained conformational searches were run using the AMBER* force field augmented by MNDO derived parameters for the Neu5Ac anomeric torsion, the GB/SA water solvation model, and the MC/EM alogorithm; extended (10–12 ns) dynamic simulations in GB/SA water were performed with the MC/SD protocol, and the stored structures were minimized. The overall mobility of the Neu5Acα2,3Gal linkage and the position of its minimum energy conformation have been shown to depend mainly on the presence or the absence of a GalNAc residue at the adjacent position. The best quantitative agreement with the available NOE data was achieved after minimization of the structures stored during the MC/SD dynamic runs. The latter protocol appears to reproduce satisfactorily the available experimental data, and can be used with confidence to build three-dimensional models of ganglioside headgroups.

Keywords: **ganglioside conformation, NMR, molecular mechanics, molecular dynamics**

Introduction

Gangliosides are a family of glycosphingolipids characterized by the presence of one or more residues of sialic acid. They are important constituents of biological membranes, particularly in the nervous system, where they participate in a wide array of biological processes. These include recognition of hormones and bacterial or viral toxins, cell growth and differentiation, and cell–cell interaction [1–3]. Many of these processes involve a carbohydrate-binding protein, which interacts with a high degree of specificity with ganglioside head groups of defined sequence. A complete understanding of gangliosides function in such recognition processes will require knowledge of the three-dimensional structures of their oligosaccharide moieties.

The conformation of various ganglioside head groups (e.g. GM1, GM2, GM3, GM4 and asialo-GM1 (GA1) oligosaccharides) has been studied by a combination of NMR spectroscopy and theoretical calculations [4]. NOE investigations have yielded information on proton spatial proximity [5–10]; ^{13}C spin relaxation time measurements have determined the local relative mobility of the various sugar residues [11], and finally ^{13}C and ^{2}H-NMR spectroscopy of model membranes with a low concentration of inserted gangliosides have been used to study the orientation of the sugar rings in such biologically relevant model systems [12–15].

NMR analysis has generally been followed by force field calculations of energetically preferred 3D conformations [4–12]. Calculations have been performed at various levels of complexity and with many force fields. The early HSEA grid searches [5,7,16,17] have been followed by conformational analyses including NMR constraints [6,9,18]. Unconstrained conformational searches have become feasible thanks to improved parameters for the sialic acid anomeric linkage [19], and finally molecular dynamics simulations have been performed [6,20]. In some instances, water solvation has also been included by implicit [19] or explicit [6,20] models.

However, many questions remain on the overall backbone conformation of these oligosaccharides and on their flexibility. In fact, as for many other carbohydrates, the NMR spectroscopic studies of gangliosides tend to yield a limited number of detectable experimental constraints. At the same time, the well-known difficulties in the computational treatment of carbohydrates [21] and the uncertainties in correlating the magnitudes of the available NOE contacts with internuclear distances [22] make a definite determination of ganglioside head group conformation hard to access.

*To whom correspondence should be addressed: A. Bernardi, L. Raimondi

These difficulties hamper the full understanding of ganglioside function at the molecular level and are a real roadblock in the process of rationally designing functional mimics of these molecules [23,24]. In this respect, the ideal computational protocol should include fully-unconstrained conformational search capabilities, for 3D-shape prediction of designed candidates before their synthesis, should be fast and reliable, adequately accounting for flexibility, and including a fast and accurate solvation treatment.

In the course of a program directed toward the design and synthesis of mimics of ganglioside GM1 [23], we developed a set of AMBER-type parameters for the anomeric torsion of α-sialyl glycosides [19]. They were used in the context of a molecular mechanics protocol based on a stochastic search of conformational space (Monte Carlo/Energy Minimization: MC/EM) that was found to satisfactorily reproduce the solution structure of GM1, as determined by NMR experiments. The same protocol was then applied with good results to the modeling of GM2 and of a structural analogue thereof (6′-GM2) [8]. In the present paper the study is extended to include ganglioside GM4 headgroup, and results obtained from extended (10–12 ns) dynamic simulations conducted on GM1, GM2, 6′-GM2 and GM4 oligosaccharides (Chart 1) with the highly efficient Still-Guarnieri Monte Carlo/Stochastic Dynamics (MC/SD) algorithm [25,26]. In all cases, water solvation was accounted for by the implicit Generalized Born/Surface Area (GB/SA) model [27] included in MacroModel [28]. The average interproton distances calculated as $<r^{-6}>^{-1/6}$ are compared with the experimental distances derived from NOE measurements. The experimental data for GM1, GM2 and 6′-GM2 were obtained in our laboratories for monomeric gangliosides in organic solvent (DMSO) (most of these data have already been published) [8,9] and for gangliosides in small micelles in water solution [10]. The glycosidic bond flexibility, as described by the computational model, is also discussed in the light of ^{13}C relaxation time measurements on GD1a-containing small DPC micelles in water [11]. The results show that a protocol based on MC/SD calculations

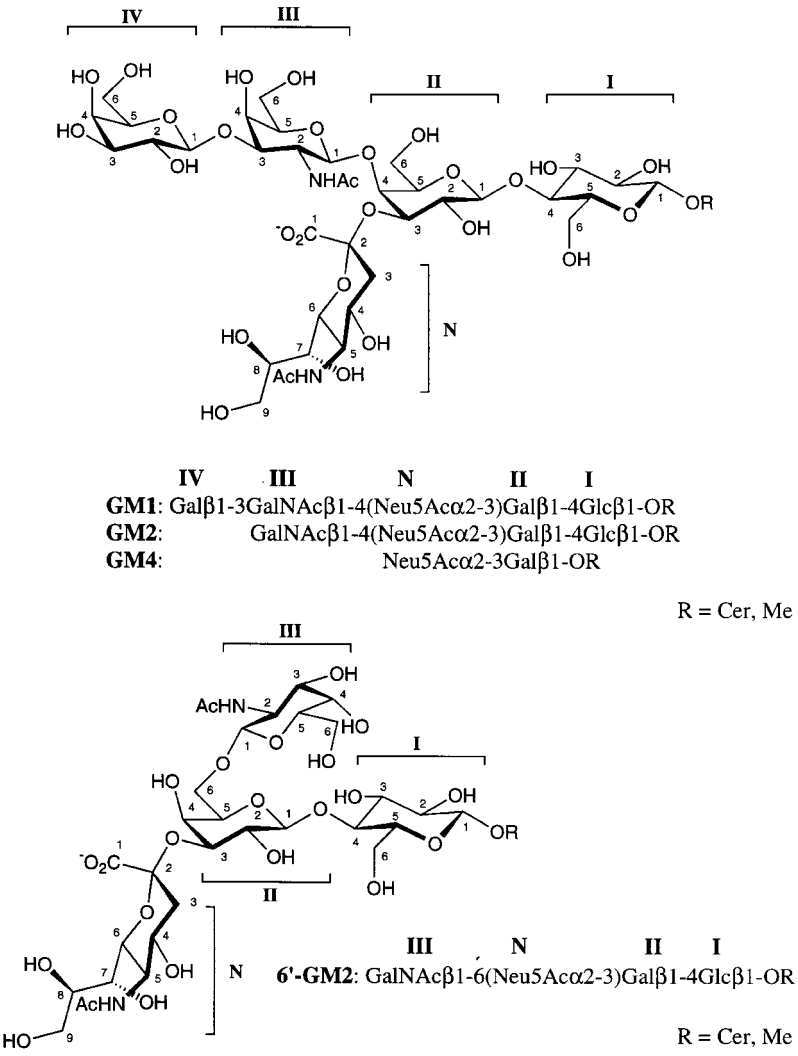

Chart 1. Gangliosides GM1, GM2, GM4 and 6′-GM2 structures and residues numbering.

followed by minimization of the conformers stored during the simulation yields the best agreement with the experimental data, and may be used with some confidence to build computational models of the ganglioside headgroups.

Computational methods

All calculations were run on an O2 SGI workstation with MacroModel/Batchmin 5.5 [28], using the AMBER* force field that contains the high quality parameters for pyranoses recently developed by Still and Senderowitz [29]. All calculations were carried out using the GB/SA water solvation model of MacroModel [27]. This model treats the solvent as an analytical continuum starting near the van der Waals surface of the solute, and uses a dielectric constant of 78 for the bulk water and 1 for the molecule. Extended nonbonded cutoff distances were used (see below). To simplify the computational problem, the ceramide chain was substituted in all calculations by a methyl group (Chart 1).

MNDO-derived parameters were included for the sialic acid anomeric torsions [19,30]. An additional substructure was included to account for the *anti* preference of the H−N−C−H dihedral angle in the sialic acid, a preference not correctly reproduced by AMBER*. MNDO calculations were performed *in vacuo* on equatorial 3-acetamidotetrahydropyrane and on diequatorial 2-methyl- and 4-hydroxy-3-acetamidotetrahydropyrane as model systems for the Neu5Ac residue (Chart 2). Standard procedures, as implemented in MOPAC 6.0 [31] were employed: geometries were optimized with the eigenvalue-following (EF) procedure and molecular mechanics correction for the acetamido moiety (MMOK); minima were characterized as such by a FORCE calculation. Drive options were used to locate all accessible conformations on the potential energy surface in order to evaluate the *syn*/*anti* preference for the acetamido residue. The H−N−C−H *anti* conformation was always favored over the *syn* one by 1.5–1.9 kcal/mol. On the basis of this preference, a suitable substructure (see Chart 2) was included in AMBER*.

MC/EM procedures. The conformational searches were carried out using the usage directed MC/EM procedure [32]. All the extra-annular bonds of the sugars that can undergo free rotation, except the C−OH bonds, were used as torsional variables in the MC steps. 10,000 MC/EM steps were performed for GM4, 15,000 for GM2, and 20,000 for the more flexible 6′-GM2 as well as for GM1. Previous studies on GM1 [19] had shown that AMBER* in GB/SA water overestimates the stability of *gauche* conformations for the C_7-C_8 diol in the Neu5Ac side chain, compared to experimental data which are consistent with an essentially *anti* conformation [4,7,9,33]. It was found that a good solution to this problem consists in starting the MC search for GM1 with a 7,8-*anti* conformer and not including the C_7-C_8 bond in the variable list. Conformational filtering (TORC) was also used to screen out *gauche* rotamers during the search [34]. The united atom version of AMBER* was used for the initial search. Energy minimization was performed using the Truncated Newton Conjugate Gradient (TNCC) procedure [35], and was terminated either after 500 iterations or when the energy gradient RMS fell below 0.1 kJ/mol Å. All conformers that differed from the global minimum energy conformation by no more than 50 kJ/mol were saved. Duplicate conformations, as defined by RMS comparison of all the heavy atoms, were discarded. After addition of explicit H atoms on the sugar, they were subjected to further energy minimization to reduce the energy gradient RMS to 0.01 kJ/mol Å. All MC/EM calculations were run with a van der Waals cutoff of 8.0 Å and an electrostatic cutoff of 20.0 Å. This protocol had been previously used for GM1 with good results [34]. The calculated distances as reported in Tables 1–4 were obtained as $r = \langle r^{-6} \rangle^{-1/6}$, where $\langle r^{-6} \rangle$ is the Boltzmann average of the r_i^{-6} of the individual conformations within 10 kJ/mol from the global minimum.

MC/SD simulations. For the MC/SD dynamic simulations van der Waals and electrostatic cutoffs of 25 Å, together with an hydrogen bond cutoff of 15 Å were used. This extension of the standard MacroModel/Batchmin values (8, 20 and 4 Å,

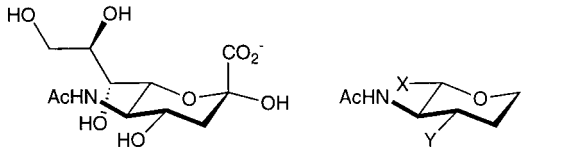

Neuraminic Acid

model systems
X = H, Me; Y = H, OH

```
-3
 C  3acetammidoTHP
 9  O3-CT-CT(-N2)-CT-CB-CT-1
-2
 4  5  3  4  C2     1.0000   0.3000   0.0000
 4  2  3  4  C2     1.3000   0.0000   0.0000
 4  H3 4  3  H1     0.0000   0.5000   0.0000
```

Chart 2. MNDO-based AMBER* substructure for Neu5Ac acetamido torsion.

Table 1. GM1: experimental and calculated interproton distances (Å).[a,b]

Entry	*Distances*	*Experimental* (DMSO)*	*Experimental** (D_2O)*	*MC/EM* $<r^{-6}>^{-1/6}$	*MC/SD* $<r^{-6}>^{-1/6}$	*MC + MC/SD* $<r^{-6}>^{-1/6}$
1	H1(IV)-H3(III)	2.5	ov	2.3	2.3	2.3
2	H1(IV)-H2(III)	3.5	3.0	4.0	4.1	4.2
3	H1(IV)-H4(III)	3.5	ov	3.8	3.4	3.8
4	H1(IV)-Ac(III)	3.8	nd	3.8	4.1	4.2
5	H1(IV)-NH(III)	3.5	3.0	3.7	3.4	3.8
6	H8(N)-H3(II)	nd	nd	3.6	3.3	4.0
7	OH8(N)-H3(II)	nd	nd	–	4.5	4.6
8	H3ax(N)-H3(II)	2.1	2.4	2.3	2.7	2.6
9	H3eq(N)-H3(II)	nd	spin diffusion	3.6	3.9	3.6
10	H3ax(N)-OH2(II)	3.2	3.4	–	2.9	3.1
11	H3eq(N)-OH2(II)	2.9	nd	–	3.4	3.2
12	H8(N)-H1(III)	3.1	ov+	2.9	3.6	2.7
13	OH8(N)-H1(III)	2.6	2.9	–	4.4	3.0
14	OH8(N)-H5(III)	3.5	ov+	–	4.2	2.9
15	OH8(N)-NH(III)	nd	3.6	–	6.3	4.5
16	H1(III)-H4(II)	2.2	2.4	2.2	2.3	2.0
17	NH(III)-H2(II)	3.6	3.4	2.8	3.0	3.0
18	Ac(III)-H2(II)	3.1	2.9	3.4	3.5	3.9
19	Ac(III)-OH2(II)	3.7	4.0	–	4.1	4.3
20	H1(II)-H4(I)	2.4	ov	2.4	2.3	2.3
21	H1(II)-H6(I)	3.1	ov	3.2	2.9	3.1
22	H1(II)-H6′(I)	nd	ov	3.1	2.9	3.0
23	H1(II)-H3(I)	ov+	ov	3.4	4.1	4.5
24	H1(II)-OH3(I)	3.3	nd+	–	3.4	3.4
25	H1(II)-OH6(I)	>4	nd+	–	3.8	4.2
26	OH2(II)-H6(I)	3.6	nd+	–	3.7	3.9
27	OH2(II)-H6′(I)	3.4	nd+	–	3.2	3.1
28	OH2(II)-OH3(I)	3.5	nd+	–	4.9	4.8
29	OH2(II)-OH6(I)	>4	nd+	–	3.7	3.2

[a]Residues are indicated as shown in Chart 1.
[b]The distances obtained from conformational searches (MC/EM) and after minimization of the structures stored during the MC/SD runs (MC + MC/SD) are calculated using the structures accessible in the first 10 kJ/mol. MC/SD distances are obtained by distance monitoring (MDDI) during the dynamics runs.
*Data from ref. 9.
**Data from ref. 10.
[nd]Not detected signals.
[nd+]Not detected due to undetectable OH in micelle.
[ov]Distance not evaluated due to signal overlap.
[ov+]Interaction not proved due to strong signal overlap.

respectively) slowed the calculation, but allowed for smoother convergence, avoiding the strong increments of the energy that can arise from significant conformational changes.

The dynamic simulations were run using the AMBER* all-atom force field. Flat bottom constraints (V_1 force constant = 1000 kJ/mol) were introduced for the C_6-C_7 ($-60° \pm 30°$) and C_7-C_8 ($180° \pm 30°$) dihedrals of the Neu5Ac moiety, in order to maintain the known conformation of the side chain. With the exception of constrained C_6-C_7 dihedral, the same degrees of freedom of the MC/EM searches were used in the MC/SD runs.

All MC/SD simulations were performed at the temperature of the corresponding NMR experiments (300–311 K), with a dynamic timestep of 1.5 fs and a bath constant τ of 0.2 ps. Typically, two runs of 5 ns each were performed, starting from two conformations of the oligosaccharides, selected from the MC/EM outputs, which differed at the Neu5Acα2-3Gal linkage. The Monte Carlo acceptance ratio was about 3%; each accepted MC step was followed by an SD step. The total time of simulation was 5 ns for GM4 and 10–12 ns for the other saccharides; structures were sampled every 2 ps. Convergence was checked by monitoring both energetic and geometrical parameters. In general, when the simulations were stopped, the interproton distances and the conformer populations determined by each run differed by no more than 0.1 Å and 5–6%, respectively. The distances as reported in Tables 1–4 were evaluated from $<r^{-6}>$ monitored during the simulation (option MDDI of Batchmin).

Table 2. GM2: experimental and calculated interproton distances (Å).[a,b]

Entry	*Distance*	*Experimental* (DMSO)*	*MC/EM* $<r^{-6}>^{-1/6}$	*MC/SD* $<r^{-6}>^{-1/6}$	*MC + MC/SD* $<r^{-6}>^{-1/6}$
1	H8(N)-H3(II)	nd	3.7	3.3	3.7
2	OH8(N)-H3(II)	4**	–	4.2	4.1
3	H3ax(N)-H3(II)	2.4	2.3	2.7	2.3
4	H3eq(N)-H3(II)	nd	3.6	3.9	3.6
5	H3ax(N)-OH2(II)	3.6	–	2.9	3.3
6	H3eq(N)-OH2(II)	3.4	–	3.5	3.5
7	H8(N)-H1(III)	2.7	2.8	3.8	2.8
8	OH8(N)-H1(III)	2.6	–	4.7	3.0
9	OH8(N)-H5(III)	3.3	–	4.3	2.9
10	OH8(N)-NH(III)	3.8	–	6.6	4.6
11	H1(III)-H4(II)	2.3	2.2	2.3	2.2
12	NH(III)-H2(II)	3.4	2.8	2.9	2.9
13	Ac(III)-H2(II)	3.6	3.8	3.6	3.4
14	Ac(III)-OH2(II)	3.9	–	4.2	3.8
15	H1(II)-H4(I)	ov	2.9	2.3	2.3
16	H1(II)-H6(I)	3	3.7	2.9	3.1
17	H1(II)-H6′(I)	nd	3.6	2.9	3.1
18	H1(II)-H3(I)	ov+	4.3	3.9	4.5
19	H1(II)-OH3(I)	3.2	–	3.4	3.4
20	H1(II)-OH6(I)	nd	–	3.9	4.4
21	OH2(II)-H6(I)	3.1	–	3.2	2.9
22	OH2(II)-H6′(I)	3.1	–	3.7	3.6
23	OH2(II)-OH3(I)	3.9	–	4.8	4.8
24	OH2(II)-OH6(I)	3.7	–	3.8	3.7

[a]Residues are indicated as shown in Chart 1.
[b]The distances obtained from conformational searches (MC/EM) and after minimization of the structures stored during the MC/SD runs (MC + MC/SD) are calculated using the structures accessible in the first 10 kJ/mol. MC/SD distances are obtained by distance monitoring (MDDI) during the dynamics runs.
[nd]Not detected signals.
[ov]Distance not evaluated due to signal overlap.
[ov+]Interaction not proved due to strong signal overlap.
*Data from ref. 8.
**Neu5AcOH8-GalH3 interaction was detected very flebile only in two Roesy experiments at 200 ms mixing time only for GM2 ganglioside.

Table 3. 6′-GM2: experimental and calculated interproton distances (Å).[a,b]

Entry	*Distance*	*Experimental* (DMSO)*	*MC/EM* $<r^{-6}>^{-1/6}$	*MC/SD* $<r^{-6}>^{-1/6}$	*MC + MC/SD* $<r^{-6}>^{-1/6}$
1	H8(N)-H3(II)	3.2	2.7	3.3	2.9
2	OH8(N)-H3(II)	3.0	–	4.4	3.2
3	H3ax(N)-H3(II)	nd	4.2	3.1	3.9
4	H1(III)-H6′(II)	2.8	2.5	2.5	2.4
5	H1(III)-H6(II)	3.0	2.7	2.8	3.0
6	NH(III)-OH3(I)	3.4	–	2.9	2.7
7	H1(II)-H4(I)	ov	2.4	2.3	2.3
8	H1(II)-H6(I)	3.3	3.1	2.9	3.1
9	H1(II)-H6′(I)	3.1	2.8	2.9	2.9
10	H1(II)-H3(I)	2.4	2.9	4.1	3.5
11	H1(II)-OH3(I)	2.8	–	3.2	3.3
12	H6(II)-OH3(I)	4.0	–	4.2	3.5

[a]Residues are indicated as shown in Chart 1.
[b]The distances obtained from conformational searches (MC/EM) and after minimization of the structures stored during the MC/SD runs (MC + MC/SD) are calculated using the structures accessible in the first 10 kJ/mol. MC/SD distances are obtained by distance monitoring (MDDI) during the dynamics runs.
[nd]Not detected signals.
[ov]Distance not evaluated due to signal overlap.
*Data from ref. 8.

Table 4. GM4: calculated interproton distances (Å).[a,b]

Entry	*Distances*	*Experimental** *(DMSO)*	*MC/EM* $<r^{-6}>^{-1/6}$	*MC/SD* $<r^{-6}>^{-1/6}$	*MC + MC/SD* $<r^{-6}>^{-1/6}$
1	H8(N)-H3(II)	d	3.4	3.3	3.1
2	OH8(N)-H3(II)	nd	–	4.5	3.4
3	H3ax(N)-H3(II)	d	3.5	3.1	3.5
4	H3eq(N)-H3(II)	d	4.4	4.1	4.4
5	H8(N)-OH2(II)	nd	–	3.7	3.4
6	OH8(N)-OH2(II)	nd	–	5.7	4.6
7	H8(N)-H4(II)	d	3.8	3.2	3.2
8	H8(N)-H1(II)	d	4.3	4.4	4.0
9	H3ax(N)-H4(II)	d	4.9	4.6	5.0
10	H3eq(N)-H4(II)	d	4.8	4.7	4.8

[a]Residues are indicated as shown in Chart 1.
[b]The distances obtained from conformational searches (MC/EM) and after minimization of the structures stored during the MC/SD runs (MC + MC/SD) are calculated using the structures accessible in the first 13 kJ/mol. MC/SD distances are obtained by distance monitoring (MDDI) during the dynamics runs.
*Data from ref. 5.
[d]Detected.
[nd]Not detected.

Minimization of the MC + MC/SD structures. All structures sampled during the MC/SD simulations were subjected to energy minimization together with those derived from the MC/EM runs, to give a final picture of all minimum energy conformations for the different energy wells. The minimization procedure was the same as described in the MC/EM section (see above). After minimization and elimination of duplicate conformers, additional filtering was necessary to screen out unwanted C_7-C_8 gauche rotamers in the Neu5Ac side chain, derived from the unconstrained minimization of MC/SD sampled conformations. Distances are reported in Tables 1–4, and were calculated as described for the MC/EM calculations.

Results and discussion

MC/EM

All molecules were initially studied by extensive MC/EM conformational searches, using the continuum GB/SA solvation model to mimic the aqueous environment. The C−OH bonds were not included in the list of the explicit torsional variables. Previous studies [8,19,23,34] had shown that under these conditions the conformational space available to oligosaccharides is exhaustively and more efficiently sampled. Indeed, when the C−OH bonds are included in the variable list, the efficiency of the search is greatly reduced, because the number of degrees of freedom to be sampled is enormously expanded. The minimum energy conformations found during the search were compared for heavy atom RMS deviation. Thus multiple copies of molecular conformations which differ only by H-bonding patterns were screened out, and only the lowest energy ones were kept as representative. This choice, which appears to be computationally convenient, was further validated by comparison with the results obtained after the MC/SD dynamic runs (*vide infra*). In fact, the network of intramolecular H bonds is explored very efficiently during the dynamic simulations, owing to the intrinsic low barriers of breaking and forming H bonds. The results obtained by the two methods will be compared in detail further on, but the main conclusion was that the MC/EM searches had located all the same backbone conformations sampled by the dynamic runs, i.e. no new significant conformations were found by the dynamic simulations. This can also be seen by comparing the φ, ψ plots of Figures 1–4. In general, energy minimization of the conformers stored during the dynamic simulations led to minima which were lower in energy than those found by MC/EM, basically due to modifications of the hydrogen bond network. However, very little, if any, reordering of the overall molecular conformations was obtained (see below the MC + MC/SD section).

A fair reproduction of the 3D structure of all the molecules studied was obtained, as judged by comparison with the NMR data. All Tables and Figures refer to the lowest energy conformations within the first 10 kJ/mol (13 kJ/mol for GM4) from the global minimum of the oligosaccharidic portion of the gangliosides (114 structures for GM2, 31 structures for GM1 and 52 for 6′-GM2 within 10 kJ/mol; 142 for GM4 within 13 kJ/mol). Interproton distances were estimated as $<r^{-6}>^{-1/6}$ Boltzmann averages over the accessible conformations within 10 (or 13) kJ/mol from the global minimum, and showed a good agreement with experimental distances measured by NOE (see Tables 1–4). For the reasons outlined above, distances involving oxygen-bound protons were not considered to be significant for these types of calculations, and were not included in the Tables.

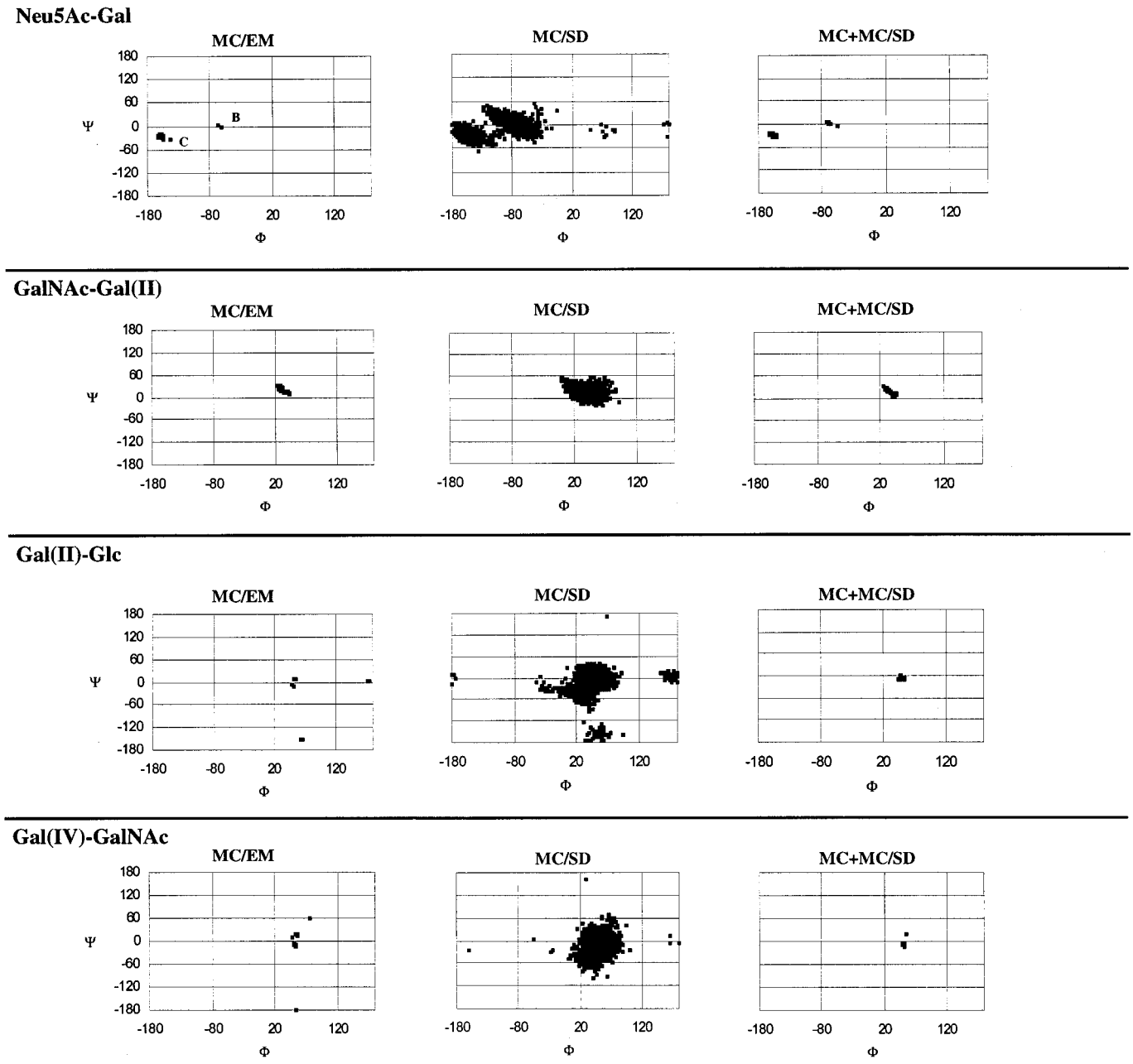

Figure 1. GM1: φ, ψ maps of the glycosidic torsions calculated by MC, MC/SD dynamic simulation and minimization of the MC + MC/SD structures. MC and MC + MC/SD data refer to the accessible conformations within the first 10 kJ/mol from the global minimum. MC/SD maps consist of 2500 sampled structures derived from a run of 5000 ps duration.

Generally speaking, the experiments find that the ganglioside headgroups can be broken down into two areas, a so-called "core trisaccharide", the GalNAcβ1-4(Neu5Acα2-3)Gal trisaccharide, which is found to be very little flexible, and the more mobile regions corresponding to the external sugars at both ends of the headgroup, which include the Galβ1-4Glc linkage, and the Galβ1-3GalNAc linkage of GM1. Interestingly, gangliosides that are not branched at the Gal moiety, such as GM3 and GM4, show a significant flexibility of the Neu5Acα2-3Gal linkage, which appears by NMR to freely sample two or more conformations. The same high mobility of the Neu5Acα2-3Gal linkage is observed in the 6′-GM2 headgroup, which also features a 4-unsubstituted Gal moiety [8]. Thus, the rigidity of the core trisaccharide appears to be related to the 3,4 disubstitution of the central Gal residue.

This general situation is reproduced rather well by the MC calculations. Inspection of Figures 1–4 shows that the MC φ, ψ maps feature 1 or 2 energy minima for the core glycosidic bonds (Neu5Acα2-3Gal and GalNAcβ1-4Gal) of GM1 (Figure 1) and GM2 (Figure 2), and multiple minima for 6′-GM2 (Figure 3),

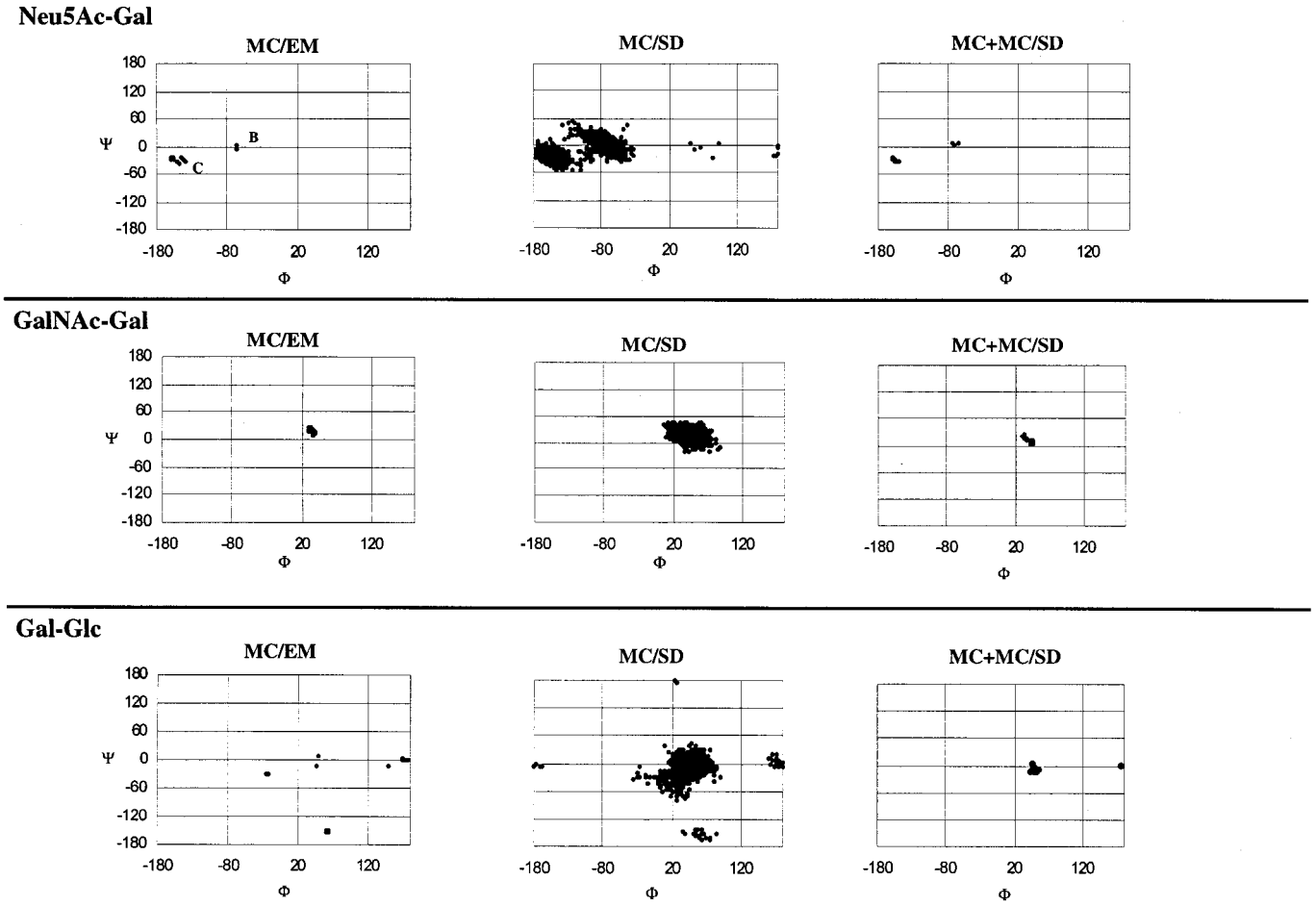

Figure 2. GM2: φ, ψ maps of the glycosidic torsions calculated by MC, MC/SD dynamic simulation and minimization of the MC + MC/SD structures. MC and MC + MC/SD data refer to the accessible conformations within the first 10 kJ/mol from the global minimum. MC/SD maps consist of 2000 sampled structures derived from two runs of 3000 ps duration each.

GM4 (Figure 4) and for the external residues of GM2 and GM1. A more detailed analysis will be conducted taking into account each glycosidic linkage and starting from the more flexible ones.

Galβ1-4Glc. The constraints dictated by the NOE measurements for the Galβ1-4Glc moiety are very weak (see Table 1, entries 20–23; Table 2, entries 15–18; Table 3, entries 7–10), and do not allow to infer a single, preferred conformation. Previous investigations [4,6,9] suggested that these bonds may sample three or four different low-energy conformations. The MC calculations do find the linkage quite flexible, but they don't seem to fully reproduce the available experimental data.

For GM1 and GM2 a high flexibility of the Galβ1-4Glc bond was calculated. Four main conformations were found for GM2 at a glycosidic angles φ, ψ 173°, 1° (global minimum), 46°, −11° (1 kJ/mol); −25°, −28° (6.5 kJ/mol) and 61°, −152° (7 kJ/mol) and three for GM1 at φ, ψ 49°, −1° (global minimum); 173°, 1° (2 kJ/mol) and 62°, −153° (6.5 kJ/mol). The experiments show that the H1 proton of the Gal moiety of both GM2 and GM1 is in NOE contact with GlcH4 and only one of the two diastereotopic GlcH6 protons. This latter feature is not reproduced by the calculations, which yield short distances with both the GlcH6 protons (Table 1, entries 21 and 22; Table 2, entries 16 and 17).

The Galβ1-4Glc glycosidic bond in 6′-GM2 displays conformational properties rather different from those of the other gangliosides, and only two minima were located at φ, ψ 47°, 6° (global minimum) and 55°, −160° (0.84 kJ/mol). The 173°, 1° conformation, which is largely populated in GM1 and GM2, appears to be missing. The two minima are characterized by a long (4.5 Å) or short (2.2 Å) GalH1-GlcH3 distance, respectively. Boltzmann averaging of the calculated distances over the first 52 conformations yields a value of 2.9 Å, in fair agreement with the observed (2.4 Å) one (Table 3, entry 10). The reduced mobility of the Galβ1-4Glc glycosidic bond in 6′-GM2 compared to GM2 may be caused by the GalNAc residue, which, being moved from the position 4 of the Gal ring in GM2 to the position 6 in 6′-GM2, can hinder some of the available space. Indeed, the proximity of the GalNAc and Glc residues in 6′-GM2 is confirmed by

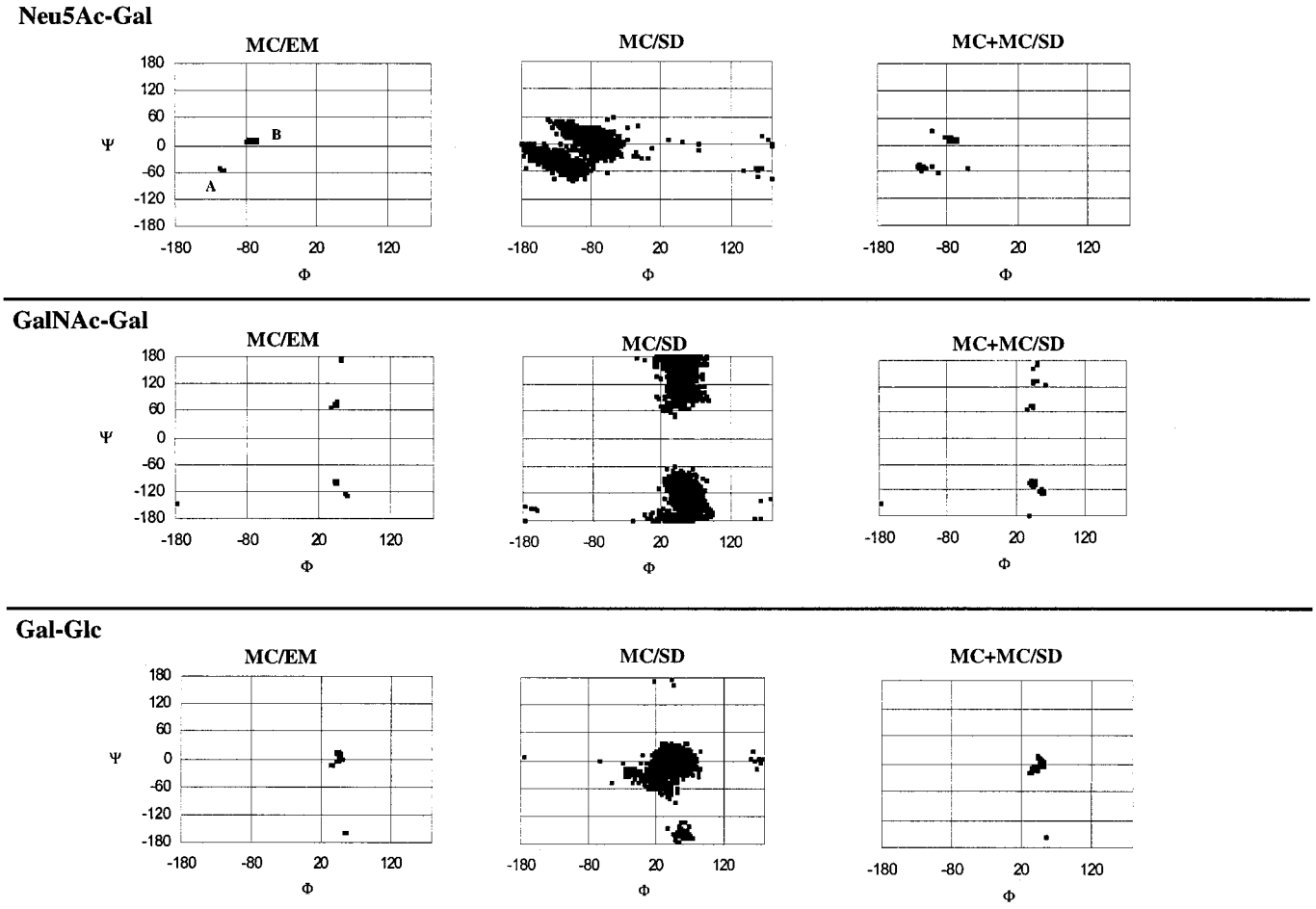

Figure 3. 6′-GM2: φ, ψ maps of the glycosidic torsions calculated by MC, MC/SD dynamic simulation and minimization of the MC + MC/SD structures. MC and MC + MC/SD data refer to the accessible conformations within the first 10 kJ/mol from the global minimum. MC/SD maps consist of 5000 sampled structures derived from two runs of 5000 ps duration each.

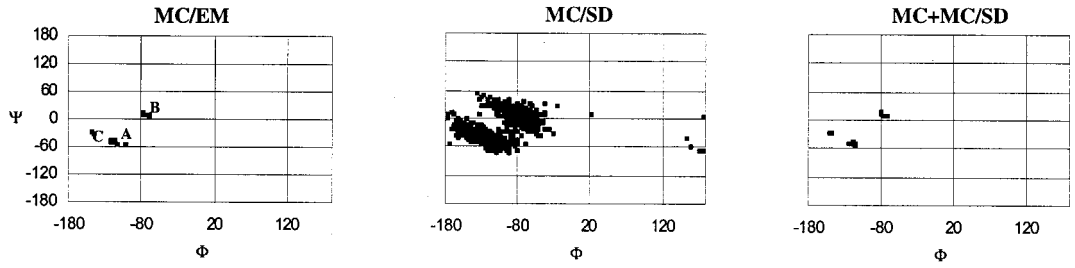

Figure 4. GM4: φ, ψ maps of the Neu5Aca2-3Gal glycosidic torsion calculated by MC, MC/SD dynamic simulation and MC + MC/SD final minimization. MC and MC + MC/SD data refer to the accessible conformations within the first 13 kJ/mol from the global minimum. MC/SD map consists of 1000 sampled structures derived from a run of 2500 ps duration.

the ROESY spectra, which show a GalNAcNH-GlcOH3 interaction (Table 3, entry 6).

Galβ1-3GalNAc. The Galβ1-3GalNAc linkage of GM1 mainly populates a single energy well at glycosidic angles φ, ψ 53°, 3° (Fig. 1). Two other unique conformations (totally less than 4% of population) were found, one 5.7 kJ/mol higher in energy from the minimum (at φ, ψ 76°, 61°), and the other with glycosidic angles 54°, −180° and $\Delta E = 6.3$ kJ/mol. It was previously suggested [9] that this linkage would sample two conformations with ψ differing by at least 70° to account for the detection of the "incompatible" GalH1-GalNAcH2 and GalH1-GalNAcH4 NOE interactions. The MC calculations suggest that rather than two individual conformations a single, broad energy minimum may exist and explain the NOE data. Indeed, the calculated energy surface does let the

linkage sample the two contacts, even if the experimental distances are not exactly reproduced (Table 1, entries 2 and 3). It may be noted that in the X-ray structure of the complex formed by GM1 and the toxin of *Vibrio Cholerae* (CT), the Galβ1-3GalNAc bond was found to assume φ, ψ $50^\circ \pm 10^\circ$, $0^\circ \pm 10^\circ$ [36].

GalNAcβ1-4Gal. Moving to the core trisaccharide, the maps of Figures 1 and 2 show that the GalNAcβ1-4Gal glycosidic bond of GM1 and GM2 adopts a very stable conformation. For both GM2 and GM1 the calculations find a single broad low energy well around glycosidic angles φ, ψ 31°, 18°. A strong interaction of the GalNAc anomeric proton with GalH4 is the only trans-glycosidic interaction detected by NMR (Table 1, entry 16, and Table 2, entry 11). NOE contacts are also observed between GalNAcNH-GalH2, GalNAcMe-GalH2 and GalNAcMe-GalOH2. All data fit the single conformation calculated (see Tables 1 and 2 for distance comparison). It has been proposed that the low mobility of the ganglioside core GalNAcβ1-4(Neu5Acα2-3)Gal is partly due to interactions between the GalNAc and Neu5Ac residues [7–11,37]. However, it is interesting to note that the scarce flexibility of the GalNAcβ1-4Gal linkage was experimentally observed also in asialo-GM1 [15] (Brocca P. *et al*., unpublished results), where the NOE pattern for the GalNAc protons are totally unaffected by the absence of sialic acid. The hypothesis that this reduced flexibility may be an intrinsic characteristic of 1-3 substituted GalNAc residues deserves further investigations.

GalNAcβ1-6Gal. Not surprisingly, the GalNAcβ1-6Gal linkage in 6′-GM2 was found to be more flexible (Figure 3). It appears to be freely rotating around the C_6–O_6 bond (ψ torsion), whereas the anomeric torsion φ is well defined around 45°. This agrees with experimental evidence indicating at least two sampled conformations for this linkage, as suggested by the simultaneous presence of the mutually exclusive GalNAcNH-GlcOH3 and GalNAcH1-GalH6 and H6′ NOE contacts (Table 3 entries 4–6) [8].

Neu5Acα2-3Gal. The conformation of the glycosidic bond Neu5Acα2-3Gal was crucial in the present study. The description of this part of the molecules is critically dependent on the anomeric torsion parameters that we obtained from semiempirical calculations [19]. Previous calculations using the MM2 force field had located three distinct allowed conformations for this linkage in GM3 [6] and in the Neu5Acα2-3Gal disaccharide (GM4 headgroup) [4,5], roughly corresponding to the three staggered orientations 60°, 180° and −60° of φ. However, the MNDO potential energy surface for the anomeric torsion of 2-methoxy-2-carbomethoxytetrahydropyrane, on which our AMBER-type parameters were based, showed a large, low-energy region for $-60^\circ \leqslant \varphi \leqslant -180^\circ$, and a high-energy plateau extending over all the positive values of φ. This is in agreement with the three allowed conformations, at φ, ψ −160°, −20°; −70°, 5° and −95°, −45°, suggested for the related structural fragment sialylα2-3N-acetyllactosamine (SLn) and for sialyl Lewis X [4,16,38].

To further complicate this issue, several of the critical interresidue NOEs observed for the Neu5Ac moiety in gangliosides refer to the H8 of the glycerol side chain. The preferred conformation of this chain can be estimated on the basis of the vicinal coupling constants $^3J_{6,7}$ and $^3J_{7,8}$ and of some intraresidue NOE contacts. All observations suggest that the glycerol side chain of 2αNeu5Ac favors an extended conformation in solution with typical H6−C6−C7−H7 (θ_1) and H7−C7−C8−H8 (θ_2) torsion angles of −60° and 180°, respectively [4,7,9,33]. This geometry may be stabilized by hydrogen bonding between the carboxyl group and the OH8, which may also account for the small temperature coefficient of this proton in all the studied gangliosides. These features could not be reproduced by totally unconstrained calculations, which found the 7-8 *gauche* conformation of the diol more stable than the *anti* one. To avoid the introduction of constraints, conformational filtering was used in the MC calculations to screen out the *gauche* rotamers (see Methods).

The conformational space available to the Neu5Acα2-3Gal linkage was initially studied for the simplest available molecule, the GM4 headgroup (Fig. 4). Three conformations were found to be accessible within 13 kJ/mol at φ, ψ −118°, −59° (A, $\Delta E = 4$ kJ/mol); −70°, 6° (B, global minimum) and −150°, −26° (C, $\Delta E = 12.7$ kJ/mol), representing about 35.0%, 64.9% and 0.1% of the total Boltzmann population. The second conformation corresponds to the B conformer of Poppe *et al*. [5] obtained by MM2 calculations, and already compared to NOE data for GM4 and the Neu5Acα2-3Gal disaccharide in water solution. Experimentally, the diagnostic NOE distances were measured for the GalH3 proton, which shows two almost equivalent contacts with the Neu5AcH8 and the Neu5AcH3ax. The former interaction can only be experienced in the B conformation (Neu5AcH8-GalH3 distance ca. 2.9 Å) whereas the latter should be absent in B (Neu5AcH3ax-GalH3 distance >4.5 Å) and should increase as the Neu5AcH3ax-GalH3 distance decreases from about 3–4 Å in A to 2.5 Å in C. A 60/40 B/A population distribution was estimated by Poppe *et al*. from the NOE data [5]. Thus the MC calculations that yield a 65/35 B/A ratio and average $<r^{-6}>^{-1/6}$ distances of 3.5 Å and 3.4 Å for Neu5AcH3ax-GalH3 and Neu5AcH8-GalH3, respectively (Table 4, entries 3 and 1), may slightly overestimate the stability of type-B family, but clearly reproduce the experimental data.

In the MC calculations of 6′-GM2 (Figure 3) [8], type-B conformations represent 94% of the total population within 10 kJ/mol from the global minimum, with glycosidic angles φ, ψ −74°, 10°. The type-A conformation was much less populated (6%) and found to be 8.2 kJ/mol higher in energy, with φ, ψ −112°, −55°. The first type-C conformation is calculated to be 23 kJ/mol higher in energy than the global minimum. Comparison between calculated and experimentally derived distances (Table 3) shows a good agreement between the two sets of data. The diagnostic GalH3-Neu5AcH8

distance (3.3 Å by NOE in DMSO) is shorter in the global minimum energy well B (2.9 Å) and longer in the type-A family (3.6 Å). The Boltzmann-averaged value of 2.7 Å is in fair agreement with the experimental data (Table 3, entry 1). The Neu5AcH3ax-GalH3 contact was not experimentally observed, in agreement with the Boltzmann-averaged value of 4.2 Å (Table 3, entry 3). Thus also for 6′-GM2 the MC/EM description of the Neu5Acα2-3Gal linkage fits quite satisfactorily with the NMR data.

These results may be compared to the description of GM3 ganglioside, as obtained by NOE-mapping and MD simulations with the CVFF force field [6]. The Neu5Acα2-3Gal linkage of this molecule appears to freely sample two different conformations at φ, ψ $-155°$, $-25°$ (C-type) and $-75°$, $10°$ (B-type), giving rise to both the Neu5AcH3ax-GalH3 and Neu5AcH8-GalH3 NOE contacts. The common feature of GM3, GM4, and 6′-GM2 is the absence of substituents at the 4 position of the Gal ring. Thus one could generalize that if the Gal-OH4 is not substituted, the Neu5Acα2-3Gal linkage can assume two or three different low-energy conformations, with a *gauche* B-type (φ, ψ $-75°$, $10°$) conformation as the global minimum, compatible with a Neu5AcH8-GalH3 short distance. The Neu5AcH3ax-GalH3 contacts can not arise from conformation B, which has typical Neu5AcH3ax-GalH3 distance >4 Å, but from conformation A (Neu5AcH3ax-GalH3 distance ca. 3.2 Å) and/or C (Neu5AcH3ax-GalH3 distance ca. 2.5 Å). Whether this NOE contact is observed (as in GM4 and GM3) or not (as in 6′-GM2) may depend on the relative ratio of A-, B-, and C-type conformations.

Moving to the Gal-OH4 branched headgroups, the MC/EM calculations on GM2 and GM1 yield lowest energy type-C conformations of the Neu5Acα2-3Gal linkage at glycosidic angles φ, ψ $-161°$, $-25°$ for GM2 and $-156°$, $-28°$ for GM1. These conformers represent the 86% and 79% of the total population of GM2 and GM1, respectively (Figures 1 and 2), while the remaining 14–21% belongs to a $-65°$, $-1°$ type-B conformation. This is a dramatic departure from the conformer distribution calculated for the headgroups discussed so far, and appears to be in substantial agreement with the available experimental data. Indeed, all results from NOE investigations of the GalNAcβ1-4(Neu5Acα2-3)Gal core in a number of gangliosides have been interpreted on the basis of a single rigid conformation of the trisaccharide featuring an *anti* type-C conformation of the Neu5Acα2-3Gal linkage. Furthermore, measurements of the ^{13}C relaxation rates on GD1a anchored to small DPC micelles in water solution [11] have shown a larger correlation time, and hence a lower flexibility, for the core GalNAcβ1-4(Neu5Acα2-3)Gal trisaccharide than for the outer Gal and Neu5Ac residues. Thus the substitution at the OH4 position of the central Gal residue in the branched gangliosides appears to substantially reduce the mobility of the Neu5Acα2-3Gal linkage, relative to GM4 and GM3, and to shift the lowest energy region of the φ, ψ maps from B ($-70°$, $-6°$) to C ($-160°$, $-25°$). It has been suggested that this shift is due to non-bonded interactions between the sialic acid and the GalNAc residues [7,11,37]. It is also tempting to speculate that the higher stability of B-type conformers in the Gal4-unsubstituted molecules may be due to electrostatic interactions between the GalOH4 and the sialic acid carboxy group.

The existence of a ganglioside rigid core has been proposed to be the reason for the resistance of GM2 and GM1 to sialidase and β-hexosaminidase [8]. The MC search finds that Neu5Acα2-3Gal in these gangliosides populates both the *anti* (C) and the *gauche* (B) conformations, conferring to the linkage a certain degree of flexibility. However, the quantitative ratio between the two conformers is harder to establish. It is possible that the stability of the *gauche* (B) Neu5Ac conformation is overestimated in this type of calculations, because the calculated Neu5AcH8-GalH3 distances (3.6 Å in GM1 and 3.7 Å in GM2) could be within the detection limits of our experiments, and yet no crosspeak is detected for this pair of protons. However, in both cases, the Neu5AcH3ax-GalH3 distance is calculated to be 1.3–1.4 Å shorter than the Neu5AcH8-GalH3 distance, and thus a qualitative agreement is undoubtedly reached with the experimental data. It is noteworthy that the Neu5AcH8-GalNAcH1 distance, which is usually taken as a gauge of the *anti* Neu5Ac conformation, is fully reproduced by the MC calculations. This suggests that the observed set of NOE contacts do not need to result from a single conformation of the ganglioside core trisaccharide, but can be qualitatively reproduced also in the presence of some residual averaging of C-type and B-type conformations, with the former being more energetically stable.

MC/SD

In order to shed some more light on the problem of the mobility of the oligosaccharides and in particular of the Neu5Acα2-3Gal linkage, molecular dynamics simulations were run for all the gangliosides under consideration. This approach should also considerably improve the description of the H-bonding network, and thus yield a more realistic view of the dynamic behavior of the molecules.

The calculations were run with the Guarnieri-Still MC/SD protocol [25]. This algorithm was designed to achieve adequate sampling of the full potential energy surface for systems having multiple conformations separated by significant energy barriers. The technique generates a canonical ensemble of molecular states by alternating Metropolis Monte Carlo (MC) and Stochastic Dynamics (SD) steps. The MC steps are used to make large random moves through conformational space, and the SD steps are used to explore each potential energy well. It has been shown that converged energies and other averaged molecular properties can be obtained by this mixed-mode method in a fraction of the time that would otherwise be required by simple SD calculations. The same MC variables were used than in the MC/EM study, except for the sialic acid side-chain torsional angles θ_1

and θ_2. These had to be restrained with flat-bottom potential terms in order to maintain the known extended conformation. Thus it was expected that all the existing minima would be reached by the MC steps, and efficiently sampled during the SD steps. In particular, the available H-bonding patterns should be exhaustively explored during the dynamics runs.

In general the conformations sampled by the dynamic calculations agree with those located by the MC search (compare the MC and MC/SD columns in Figures 1–4), in that all the MC minima appear to be sampled during the simulations, and only scattered points, if any, are found outside the MC minimum energy areas. However, some interesting observations can be made.

Galβ1-4Glc. For all the three gangliosides involved (GM2, 6′-GM2 and GM1) more than 98% of the conformers are located in a large well centered on φ, ψ $50° \pm 30°$, $0° \pm 30°$. Two more minima are populated at φ, ψ 173°, 1° and 60°, −150°. Minor differences between 6′-GM2 (Figure 3) and the other two gangliosides (Figs. 1 and 2) persist, since the former has a vanishingly small (0.3%) population at φ, ψ 180°, 0°, compared to ca. 1% of GM1 and GM2, but the overall picture is much more uniform than what expected on the basis of the MC calculations.

Galβ1-3GalNAc. The simulation confirmed the existence of a single, very large low-energy valley ($-100° \leqslant \varphi \leqslant 60°$, $10° \leqslant \psi \leqslant 100°$; Fig. 1). Within this area, the bond appears to be very flexible, and to fluctuate between local minima separated by very low barriers.

GalNAcβ1-4Gal. The simulations of GM1 and GM2 showed a single, rather compact energy well centered at $\varphi = 40°$ (Figs. 1 and 2). As in the MC calculations the GalNAcβ1-6Gal bond of 6′-GM2 appears to be much more flexible along the exo-anomeric torsion ψ, which goes from −100° to 60°, than along φ, which is fixed at about 45°.
The GalNAcH1-Gal(II)H6,6′ and GalNAcNH-GlcOH3 interactions all appear to be quite well reproduced (Table 3, entries 4–6).

Neu5Acα2-3Gal. The most puzzling differences between the dynamic calculations and the MC data concern the Neu5Acα2-3Gal bond. The MC/SD simulations of the GM4 oligosaccharide (Figure 4) show that the A(−118°, −59°) and C(−160°, −29°) minima located by the MC/EM search are not distinct, but rather belong to an ample energy valley spanning a large interval of φ, ψ values. This appears to be connected by a frequently crossed barrier to a second large area which includes the B(−70°, −6°) conformer. The population ratio of these two areas was calculated to be 45/55, still in good agreement with the experimental data of Poppe [5]. The calculated distances for the crucial interproton contacts are 3.3 Å and 3.1 Å for Neu5AcH8-GalH3 and Neu5AcH3ax-GalH3, respectively (Table 4, MC/SD column, entries 1 and 3). By MC/EM, a 65/35 B/(A + C) ratio had been evaluated which yielded distances of 3.4 Å and 3.5 Å for the two diagnostic contacts (Table 4, MC/EM column). So the Neu5AcH8-GalH3 is essentially unaffected by the method of calculation, but the MC/SD Neu5AcH3ax-GalH3 distance is significantly shorter than the MC/EM value, because of the increased statistical weight of the C conformation.

The high mobility of the Neu5Acα2-3Gal linkage for the Gal4-unsubstituted gangliosides is confirmed by the GM4 simulation, which also shows rather frequent transitions between the two populated areas (Fig. 4). In the 6′-GM2 simulations (Fig. 3) the two low-energy regions almost collapse in a single U-shaped valley, which extends to include also the C-type conformations (−160°, −29°). As a result, the predicted Neu5AcH8-GalH3 and Neu5AcH3ax-GalH3 distances become essentially equal to one another (Table 3).

A very different picture is found for the Gal4-branched gangliosides GM1 and GM2 (Figs. 1 and 2). Two low-energy regions are sampled, one corresponding to the *anti* (C-type) and one to the *gauche* (B-type) conformers. The two areas appear to be well separated, and no populations is found to correspond to the A(−118°, −59°) conformer. This situation is in agreement with the observed limited mobility of internal Neu5Acα2-3Gal bonds in disialo gangliosides [11]. However, and in contrast with the GM4 case, an increment of the B-type (*gauche*) conformation is seen, which goes from the 14–21% statistical weight of the MC data to an almost 1:1 ratio with the C (*anti*) conformation of the MC/SD maps (Figs. 1 and 2). Consistently, the MC/SD Neu5AcH3ax-GalH3 distance (typical contact of the C conformation) is somewhat longer and the Neu5AcH8-GalH3 (typical contact of the B conformation) shorter than the MC calculated distances (Table 1, entries 6 and 8; Table 2 entries 1 and 3). This increase of the *gauche* population is also reflected in the increase of the Neu5AcH8-GalNAcH1 distance (Table 1, entry 12, Table 2, entry 7) to unrealistically high values, and even above the detection threshold in the case of GM2. Furthermore, the Neu5AcOH8-GalNAcNH distance of 6–7 Å does not reproduce the experimental evidence which in all studied gangliosides detects a NOE cross peak corresponding to a distance of about 3.5–3.8 Å.

The global picture emerging from the dynamic simulations is in qualitative agreement with the MC/EM results. In fact, the Gal4-unsubstituted molecules GM4 and 6′-GM2 are still found to display two similar NOE contacts for the GalH3 proton, corresponding to distances that are both above 3 Å. On the contrary, the Gal(II) 3,4-branched molecules GM2 and GM1 are found to display two non equivalent contacts: a stronger one for the GalH3-Neu5AcH3ax distance safely below 3 Å and a weaker one for the GalH3-Neu5AcH8 distance well above 3 Å. This is the result of a fairly constant statistical weight of the B conformer (ca. 50% for all headgroups), and of a shift of the alternative conformation from A (fairly long Neu5AcH3ax-GalH3 distance) in GM4 and 6′-GM2 to C (very short Neu5AcH3ax-GalH3 distance) in GM1 and GM2. However, the overall effect of the dynamics

simulations is to reduce the agreement with the experimental data. Incomplete convergence of the calculations, although always difficult to completely rule out, does not seem a convincing explanation of these results, given the length of the simulations and the little deviations observed between the different runs (see Methods). Rather it may be noted that many of the conclusions that can be drawn are based on comparing the NOE contacts of the Neu5AcH8 proton, and hence they strongly depend on the accurate description of the Neu5Ac side chain. We have already remarked that the Neu5Ac side chain is, on the contrary, one of the critical points of the calculations, and that the dynamic simulations need to be restrained in that point in order to reproduce the pattern of the observed coupling constants. A second element to take into account is that the accuracy of the dynamic simulations will depend critically on the fine details of the potential energy surface, as it is calculated by the force field. Thus AMBER* may be well parameterized as far as the position and depth, but not the width, of the Neu5Acα2-3Gal energy minima are concerned. To test this hypothesis, the structures collected during the dynamic simulations were subjected to further minimization.

Minimization of the MC + MC/SD structures

The structures saved during the dynamic runs were energy minimized together with the minima obtained by the MC/EM calculations (see Methods). All the conformations belonging to the first 10 kJ/mol from the global minimum were saved. Torsional data for the different backbone conformations and their relative energies are collected in Table 5. In general this procedure would privilege the structures obtained from the MC/SD calculation because, once energy minimized, they usually fall into minima at lower energy than those obtained by the MC calculations alone. As previously mentioned, the energy gain appears to be related to a better description of the H bonding network, since (a part from the Galβ1-4Glc linkage) the overall backbone conformations remain essentially the same. For instance, the minimum energy structure of GM1 in the MC + MC/SD calculations is 12.7 kJ/mol lower in energy than the one obtained by MC. This ΔE depends on a different orientation of the Gal(IV) ω (C_5-C_6) dihedral angle ($-52°$ in the MC/EM, 58° in the MC + MC/SD minimum); the orientation of Neu5Ac C_8-C_9 angle also changes from 77° (MC/EM) to 170° (MC + MC/SD). This results in a change

Table 5. Torsional data for the different backbone conformations calculated by MC/EM and after minimization of the structures stored during the dynamic runs (MC + MC/SD).

	Neu5Ac-Gal(II)		*Gal(II)-Glc*		*GalNAc-Gal(II)*		*Gal(IV)-GalNAc*	
ΔE (kJ/mol)	φ_C	ψ_H	φ_H	ψ_H	φ_H	ψ_H	φ_H	ψ_H
GM1								
0.00	−158.2	−26.4	51.2	−7.1	30.4	21.1	51.9	−9.9
3.63	−67.8	1.4	48.4	−9.0	28.7	23.2	52.5	−11.7
GM2								
0.00	−157.0	−25.2	52.5	−6.4	35.1	15.3		
4.37	−67.9	1.4	48.4	−9.0	30.4	22.0		
9.90	−156.3	−28.4	24.4	−54.5	31.1	20.9		

	GalNAc-Gal(II)		
	φ_H	ω_H	ψ_C
6′-GM2			
0.00	−73.0	−53.1	−128.1
1.84	−77.2	−69.8	75.6
3.17	−75.2	−73.4	70.0
3.40	−119.7	−52.5	−127.7
3.63	−118.2	−50.5	47.2	128.9
6.89	−70.4	−54.9	172.2
7.16	−116.7	−56.3	−174.7	−108.4
7.71	−120.0	−52.5	−58.3	161.6
8.55	−70.7	−164.3	−113.4
9.32	−73.1	−177.8	−52.4	−150.2
GM4			
0.00	−74.0	−122.2	−47.9
2.22			

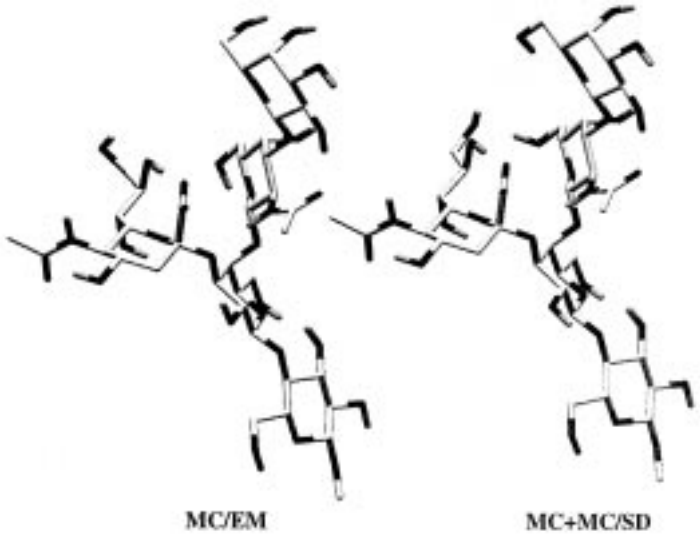

Figure 5. Comparison of GM1 global minima from MC/EM and MC + MC/SD searches.

of the hydrogen bond network: the Gal(IV)OH6-O4 hydrogen bond is lost in the new minimum energy conformation, while GalNAcOH6 and Neu5AcOH9 gain one H bond interaction each. Thus the total number of hydrogen bonds is left unchanged (Fig. 5).

The main exception is constituted by the MC + MC/SD φ, ψ maps of the Galβ1-4Glc linkage (Figures 1–3, MC + MC/SD column), which appear to be concentrated by more than 99% in the $50^\circ \pm 30^\circ$, $0^\circ \pm 30^\circ$ well. This area was the most populated by the dynamics simulation, and much of the flexibility predicted by the MC calculations (Column MC) appears to be lost. As already remarked, the experimental data on this linkage indicate that it is quite flexible and it samples different conformation. There may be various reasons for these problems in the description of the Galβ1-4Glc bond. The presence of the ceramide chain in the experimental sample, as opposed to a methyl group in the computational "sample", is likely to produce the largest effect on the conformation of the Glc residue, to which it is attached. Again, incomplete sampling of the rotamer population cannot be ruled out, particularly for such a flexible linkage.

On the contrary, once the structures are minimized, the relative populations of the A, B and C conformations of the Neu5Acα2-3Gal linkage are found to be in agreement with the experimental data and with what expected on the basis of the MC calculations (Table 6). Thus the final minimization leads to a 15/85 B/C ratio for GM2 (Figure 1) and 7/93 for GM1, in sharp contrast with the 87/13 B/A ratio found for 6′-GM2 and the 61/35/4 B/A/C ratio calculated for GM4. The description of the interproton distances is also improved, and the calculated Neu5AcH8-GalH3 distances of GM2 and GM1 move above the NOE detection threshold, in agreement with the experimental observations (Table 1, entry 1; Table 3, entry 6).

The large prevalence of the *anti* conformation of the Neu5Acα2-3Gal linkage supports the experimentally suggested notion of a fairly rigid core trisaccharide GalNAcβ1-4(Neu5Acα2-3)Gal, likely to bear functional information. However, the calculations show that the experimental data can be reproduced also if a *gauche*, less stable conformation (ca. 10% of the total population) is accounted for. The only experimental indication for the existence of a *gauche* conformation of the Neu5Acα2-3Ga linkage in GM1 or GM2 comes from a very weak NOE effect between Neu5Ac OH8 and Gal H3 detected only for GM2 and under some very defined experimental conditions (see Table 2). No analogous contact was ever detected in ganglioside GM1 spectra. Although the calculations appear to

Table 6. Relative populations of minima A, B, and C of the Neu5Acα2-3Gal linkage calculated by MC/EM and after minimization of the structures stored during the dynamic runs (MC + MC/SD).[a]

	GM1			*GM2*			*6′-GM2*			*GM4*		
Method	*A*	*B*	*C*	*A*	*B*	*C*	*A*	*B*	*C*	*A*	*B*	*C*
MC/EM	0	21	79	0	14	86	6	94	0	35	65	0
MC + MC/SD	0	7	93	0	15	85	13	87	0	35	61	4

[a]A: φ, ψ -120°, -60°; B: φ, ψ -70°, 0°; C: φ, ψ -150°, -25° (see text).

overestimate to some extent the occurrence of the B-type (*gauche*) conformation, it seems legitimate to wonder whether experiments run with higher sensitivity may not yield interesting results in this sense (for a similar situation in the sialyl Lewis X case, see ref 38).[#]

Conclusions

All available experimental data on the structure and enzymatic susceptibility of gangliosides indicate that the Gal3,4 branched headgroups of GM1 and GM2 are less mobile and less accessible to glycosidases (sialidases and hexosaminidases) than the unbranched structures of 6′-GM2 and asialo-GM2. The same different mobility is seen for internal and external sialic acid residues in disialo-gangliosides such as GD1a. The low enzymatic susceptibility of GM1 and GM2 may be explained by the steric hindrance that results from the proximity of the sialic acid and GalNAc rings in the branched structure. Steric hindrance may also be the ultimate cause of the low conformational mobility, at least of the sialic acid residue.

The calculations employing MNDO derived parameters for the sialic acid anomeric torsion, the GB/SA water solvation model, and efficient algorithms for the search of the available conformational space (MC/EM and MC/SD of MacroModel) have been able to qualitatively reproduce the available data. The overall mobility of the Neu5Acα2-3Gal linkage and the position of its minimum energy conformation have been shown to depend mainly on the presence or the absence of a GalNAc residue at the adjacent Gal4 position. The conformation of the GalNAcβ1-4Gal linkage appears to be constant in all the structures examined, and preliminary experimental (NMR) data on asialo-GM2 suggest that it is conserved also in the absence of an adjacent sialic acid substituent.

The MC/SD dynamic simulations predicted an unrealistically high flexibility of the Gal3-4 branched gangliosides GM2 and GM1, which were best described by the relative populations of their minimum energy conformations.[¶] The reason for this may be connected to the difficulties encountered in the reproduction of the known conformation of the Neu5Ac side chain. These are apparently due to the inherent tendency of AMBER* to favor the *gauche* conformation of 1,2-diols, in agreement with available high-level theoretical calculations and gas-phase experimental data [40–42]. The experimentally derived 6,7-*gauche*, 7,8-*anti* conformation can be preserved during the MC/SD run only by imposing constraints, which may alter the reproduction of the overall flexibility. However, test simulations run with different flat bottom constraints, e. g. $\pm 10°$, $\pm 30°$ or $\pm 60°$ allowed variations, yielded essentially the same anomeric distributions. More likely, the problems in the dynamic simulations depend on inaccurate parameterization of the sialic acid anomeric torsion. In fact, the MNDO potential energy surface for the $C_1-C_2-C_n-O_n$ of 2-carbomethoxy pyranose, which was used for the parameterization of the Neu5Ac φ, appears as a flat and large valley from $-180°$ to ca. $-60°$ where a steep barrier begins [19]. While the MNDO-derived AMBER* parameters allow a good reproduction of these general features, no effort was made to reproduce the fine details of the low energy area. Finally, it cannot be ruled out that differential solvation of the different conformations may play a role in determining their dynamic behavior, which the GB/SA solvation model is not fully able to reproduce, at least with the standard set of atomic charges that are used in the present work. Further work is in progress in all these directions.

The best quantitative agreement with the available NOE data, and hence the most accurate model of the headgroup conformations, appears to be achieved upon minimization of the structures stored during the MC/SD dynamic runs. Despite the drawbacks outlined before, the MC/SD dynamic simulations appear to improve the description of the systems compared to the MC/EM calculations, by allowing an accurate exploration of the H bond potential energy surface. Minimization of all the structures stored during the Monte Carlo and the dynamic runs yields a satisfactory model of the solution conformation of ganglioside headgroups, as judged by the fair reproduction of the NOE data reported in Tables 1–4. Thus, it appears that the optimal procedure for accurate modeling of this type of molecules should include the following steps: (1) MC/EM search of the major backbone conformations. This will yield the input structures for step 2. (2) Extended MC/SD simulations starting from lowest energy conformations of step 1, and storage of sampled structures. Performing multiple runs starting from different MC/EM conformations will allow to evaluate the convergence of the simulation. (3) Energy minimization of the structures sampled during step 2. The pool of minima located in steps 1 and 3 seems to yield fairly accurate representation of ganglioside headgroups.

It is noteworthy that these results were obtained with no need for experimental constraints, except than for the Neu5Ac side-chain, and thus the protocol described above should be useful as a designing tool in the rational development of ganglioside mimetics.

Acknowledgements

Support from C.N.R. (Centro Studio Sostanze Organiche Naturali and Centro Studio Sintesi Stereochimica Speciali Sistemi Organici) is gratefully acknowledged.

[#]It may also be noted that a synthetic mimic of ganglioside GM1 headgroup, which appears to interact just as strongly with cholera toxin (CT), does show interproton contacts in its ROESY spectra which are analogous to the Neu5AcH3ax-GalH3 (strong signal) and Neu5AcH8-GalH3 (weaker signal) contacts [23]. Since GM1 is known to bind CT in the Neu5aα2-3Gal *anti* conformation [36], the equal affinity of these two molecules for the toxin may be interesting to note.

[¶]Although comparison to a r^{-6} average may not be entirely correct for the molecules under study [39] the same average was used for all the computational methods involved, and the problems with the MC/SD algorithm appear to depend mainly on the fine features of the potential energy surface.

Glycosidic angles φ, ψ are defined as follows: for Galβ1-3GalNAc: φ = GalH1-GalC1-O1-GalNAcC3, ψ = GalC1-O1-GalNAcC3-GalNAcH3; for GaNAcβ1-4Gal: φ = GalNAcH1-GalNAcC1-O1-GalC4, ψ = GalNAcC1-O1-GalC4-GalH4; for 6′-GM2: GaNAcβ1-6Gal, φ = GalNAcH1-GalNAcC1-O1-GalC6, ψ = GalNAcC1-O1-GalC6-GalC5 (ω = GalH5-GalC5-GalC6-O6): for Neu5Acα2-3Gal: ψ = Neu5AcC1-Neu5AcC2-O2-GalC3, ψ = Neu5AcC2-O2-GalC3-GalH3; for Galβ1-4Glc: φ = GalH1GalC1-O1-GlcC4, ψ = GalC1-O1-GlcC4-GlcH4.

In Tables 1–4 the residues are indicated as depicted in Chart 1.

References and notes

1 Karlsson K-A, Animal glycosphingolipids as membrane attachment sites for bacteria, *Ann Rev Biochem* **58**, 309–50 (1989).

2 Hakomori S-I, Bifunctional role of glycosphingolipids, *J Biol Chem* **265**, 18713–6 (1990).

3 Nagai Y, Ganglioside reasearch: new trends and reflections, *Pure & Appl Chem* **70**, 533–8 (1998).

4 For leading references see: Rao VSR, Qasba PK, Baloyi PV, Chandrasekaran R, *Conformation of carbohydrates.* Harwood Academic Publishers (1998).

5 Poppe L, Dabrowski J, von der Lieth CW, Numata M, Ogawa T, Solution conformation of sialosylcerebroside (GM4) and its NeuAc(α2-3)Galβ sugar component, *Eur J Biochem* **180**, 337–42 (1989).

6 Siebert HC, Reuter G, Schauer R, von der Lieth CW, Dabrowski J, Solution conformation of GM3 gangliosides containing different sialic acid residues as revealed by NOE based distance mapping, molecular mechanics and molecular dynamics calculations, *Biochemistry* **31**, 6962–71 (1992).

7 Sabesan S, Block K, Lemieux RU, The conformational properties of the gangliosides GM2 and GM1 based on 1H and 13C nuclear magnetic resonance, *Can J Chem* **62**, 1034–45 (1984).

8 Li Y-T, Li S-C, Hasegawa A, Ishida H, Kiso M, Bernardi A, Brocca P, Raimondi L, Sonnino S, Structural basis for the resistance of Tay-Sachs ganglioside GM2 to enzymatic degradation, *J Biol Chem* **274**, 10014–8 (1999).

9 Acquotti D, Poppe L, Dabrowski J, von der Lieth CW, Sonnino S, Tettamanti G, Three-dimensional structure of the oligosaccharide chain of ganglioside revealed by distance mapping procedure: a rotating and laboratory frame nuclear Overhauser enhancement investigation of native glycolipid in dimethyl sulfoxide and in water-dodecylphosphocoline solution, *J Am Chem Soc* **112**, 7772–8 (1990).

10 Brocca P, Berthault P, Sonnino S, Conformation of the oligosaccharide chain of GM1 ganglioside in a carbohydrate-enriched surface, *Biophys J* **74**, 309–18 (1998).

11 Poppe L, van Halbeek H, Acquotti D, Sonnino S, Carbohydrate dynamics at a micellar surface: GD1a headgroup transformations revealed by NMR spectroscopy, *Biophys J* **66**, 1642–52 (1994).

12 Aubin Y, Ito Y, Paulson JC, Prestegard JH, Structure and dynamics of the sialic acid moiety of GM3-ganglioside at the surface of a magnetically oriented membrane, *Biochemistry* **32**, 13405–13 (1993).

13 Barber KR, Hamilton KS, Rigby AC, Grant CWM, Behaviour of complex oligosaccharides at a bilayer membrane surface probed by 2H-NMR, *Biochem Biophys Acta* **1190**, 376–84 (1994).

14 Singh DM, Shan X, Davis JH, Jones DH, Grant CWM, Oligosaccharide behavior of complex natural glycosphingolipids in multicomponent model membrane, *Biochemistry* **34**, 451–63 (1995).

15 Jones DH, Barber KR, Grant CWM, Minor influence of sialic acid on conformation of a membrane-bound oligosaccharide recognition site, *Biochemistry* **35**, 4803–11 (1996).

16 Breg J, Kroon-Batenburg LMJ, Strecker G, Montreuil J, Vliegenthart JFG, Conformational analysis of the sialylα(2-3)N-acetyllactosamine structural element occurring in glycoproteins, by two-dimensional NOE ^{1}H-NMR spectroscopy in combination with energy calculations by hard-sphere exo-anomeric and molecular mechanics force fields with H-bonding potentials, *Eur J Biochem* **178**, 727–39 (1989).

17 Sabesan S, Bock K, Paulson JC, Conformational analysis of sialyloligosaccharides, *Carb Res* **218**, 27–54 (1991).

18 Scardsale JN, Prestegard JH, Yu RK, NMR and computational studies of interaction between remote residues in gangliosides, *Biochemistry* **20**, 9843–55 (1990).

19 Bernardi A, Raimondi L, Conformational analysis of GMI oligosaccharides in water solution with a new set of parameters for the Neu5Ac moiety, *J Org Chem* **60**, 3370–7 (1995).

20 Mukhopadhyay C, Bush CA, Molecular dynamics simulations of oligosaccharides containing N-acetylneuraminic acid, *Biopolymers* **34**, 11–20 (1994).

21 Woods RJ, Computational carbohydrate chemistry: what theoretical methods can tell us, *Glycoconj J* **15**, 209–16 (1998).

22 For a discussion see: Rubinstenn G, Sinay P, Berthault P, Evidence of conformational heterogeneity for carbohydrate mimetics. NMR study of β-methyl-C-lactoside in aqueous solution, *J Phys Chem A* **101**, 2536–40 (1997).

23 Bernardi A, Checchia A, Brocca P, Sonnino S, Zuccotto F, Sugar mimics: an artificial receptor for Cholera Toxin, *J Am Chem Soc* **121**, 2032–6 (1999).

24 For a review on carbohydrate mimetics see: Sears P, Wong C-H, Carbohydrate mimetics: a new strategy for tackling the problem of carbohydrate-mediated biological recognition, *Angew Chem Int Ed* **38**, 2300–24 (1999).

25 Guarnieri F, Still WC, A rapidly convergent simulation method: mixed Monte Carlo/stochastic dynamics, *J Comput Chem* **15**, 1302–10 (1994).

26 For an application of this protocol to the study of solution conformation of oligosaccharides, see Bernardi A, Raimondi L, Zanferrari D, Conformational analysis of saccharides with Monte Carlo/stochastic dynamics simulations, *J Mol Struct (THEOCHEM)* **395–396**, 361–73 (1997).

27 Still WC. Tempzyk A, Hawley R, Hendrickson T, Semianalytical treatment of solvation for molecular mechanics and dynamics, *J Am Chem Soc* **112**, 6127–9 (1990).

28 Mohamadi F, Richards NGJ, Guida WC, Liskamp R, Lipton M, Caufield C, Chang G, Hendrickson T, Still WC, MacroModel – An integrated software system for modeling organic and bioorganic molecules using molecular mechanics, *J Comp Chem* **11**, 440–67 (1990).

29 Senderowitz H, Still WC, A quantum mechanically derived all-atom force field for pyranose oligosaccharides. AMBER* parameters and free energy simulations, *J Org Chem* **62**, 1427–38 (1997).

30 In ref. 19, additional parameters were included in the force field in an attempt to reproduce the conformational features of the Neu5Ac side chain. The problem, however, was only solved by filtering unwanted conformations (see Text), so only the anomeric parameters for the sialic acid were retained in this work.
31 Stewart JJP, MOPAC 6.0. QCPE Program N. 455 (1990).
32 Chang G, Guida WC, Still WC, An internal coordinate Monte Carlo method for searching conformational space, *J Am Chem Soc* **111**, 4379–86 (1989).
33 Brown EB, Brey WS, Weltner W Jr, Cell-surface carbohydrates and their interactions I. NMR of N-acetylneuraminic acid, *Biochim Biophys Acta* **399**, 124–30 (1975).
34 Bernardi A, Raimondi L, Zuccotto F, Simulation of protein-sugar interactions: a computational model of the complex between ganglioside GM1 and the Heat-Labile Enterotoxin of *Escherchia coli., J Med Chem* **40**, 1855–62 (1997).
35 Ponder JW, Richards FM, An efficient Newton-like method for molecular mechanics energy minimizations of large molecules, *J Comp Chem* **8**, 1016–24 (1987).
36 Merritt EA, Sarfaty S, Van den Akker F, L'Hoir C, Martial JA, Hol WGJ, Crystal structure of Cholera Toxin B-pentamer bound to receptor (GM1) pentasaccharide, *Protein Sci* **3**, 166–75 (1994).
37 Acquotti D, Cantu' L, Ragg E, Sonnino S, Geometrical and conformational properties of ganglioside GalNAc-GD1a, IV^4 GalNAcIV^3 Neu5AcII^3 Neu5AcGgOse^4 Cer, *Eur J Biochem* **225**, 271–88 (1994).
38 Harris R, Kiddle GR, Field RA, Milton MJ, Ernst B, Magnani JL, Homans W, Stable-isotope-assisted NMR studies on ^{13}C-enriched sialyl Lewis X in solution and bound to E selectin, *J Am Chem Soc* **121**, 2546–51 (1999).
39 Peters T, Meyer B, Stuike-Prill R, Somorjai R, Brisson J-R, A Monte Carlo method for conformational analysis of saccharides, *J Carboh Res* **238**, 49–73 (1993).
40 Cramer CJ, Truhlar DG, Quantum chemical correlation analysis of 1,2-ethanediol: correlation and solvation effects on the tendency to form internal hydrogen bonds in the gas phase and in aqueous solution, *J Am Chem Soc* **116**, 3892–900 (1994) and references therein.
41 Cornell WD, Cieplak P, Bayly CI, Kollman PA, Application of RESP charges to calculate conformational energies, hydrogen bond energies and free energies of solvation, *J Am Chem Soc* **115**, 9620–31 (1993).
42 Rockwell GD, Grindley TB, Conformational analysis of cyclohexane-1,2-diol derivatives and MM3 parameter improvement, *Aust J Chem* **49**, 379–90 (1996).

Received 8 February 2000, revised and accepted 8 June 2000